Polymer 214 (2021) 123249

Contents lists available at ScienceDirect

Polymer

journal homepage: http://www.elsevier.com/locate/polymer

Versatile bifunctional building block for *in situ* synthesis of sub-20 nm silver nanoparticle and selective copper deposition

Seonwoo Lee

School of Electrical and Computer Engineering, Inter-University Semiconductor Research Center, Seoul National University, Seoul, 08826, Republic of Korea

ARTICLE INFO

Keywords:
Electroless plating
Metallic grid
Transparent conducting film
Silver nanocatalyst

ABSTRACT

In this work, a new bifunctional building block is presented for the development of versatile photosensitive resists, which enable *in situ* synthesis of sub-20 nm silver nanoparticles (AgNPs). In addition, practical adaptation to a palladium (Pd)-free electroless plating process verifies the facile fabrication of a metallic grid-based transparent conductive film. The building block is an aromatic small molecule with α,β-unsaturated acryloyl group and *para*-hydroxyl group protected by an acid-labile group (i.e., Di-*tert*-dicarbonate (referred to as Boc anhydride)). Spectroscopy analysis verifies the ease of photopolymerization as well as deprotection of Boc from the *para*-hydroxyl group where plays a key role in Ag^+ reduction. The studies on plasmon absorption, morphology and elemental analysis confirm that the *in situ* synthesized AgNPs are sub-20 nm with a uniform distribution in the polymer matrix, which is important for efficient catalytic performance in electroless copper (Cu) deposition. In addition, the photosensitive resist exhibited excellent process reliability with respect to photolithographic patterning process and electroless plating under strong alkaline solutions (pH 10–12). Finally, the present work demonstrates the successful fabrication of sub-3 μm Cu metal grids on a polyethylene naphthalate (PEN) film.

1. Introduction

Noble metal nanoparticles (i.e., silver (Ag), gold (Au)) are of great interest due to their unique optical features (i.e., surface plasmon resonances (SPRs)) and remarkable catalytic activities in chemical oxidation and reduction [1–9,47–51]. Silver nanoparticles (AgNPs) are also known as an inexpensive and highly efficient alternative catalysts for palladium (Pd)-free electroless plating [10,11,13,15,20], which enables low-cost and high volume fabrication methods for structuring sub-3 μm microelectrodes used in a wide range of electronics, 3D printing as well as water splitting, etc [12,14–19,21–25].

State-of-the-art techniques for the synthesis of AgNPs in electroless plating process include (i) chemical or photoreduction of silver ions chemisorbed on grafted polymers or activated substrates [25–29], (ii) direct synthesis in functionalized host polymers (also known as *in situ* synthesis of AgNPs) [30–36,46]. Particularly in *in situ* methods, precise control of the particle size, shape and uniform distribution in the host polymer are important for high catalytic performances during electroless plating.

For the *in situ* synthesis methods, recent studies have revealed possible Ag^+ reduction mechanisms and process optimization in host polymers with functional substituents (i.e., R–OH, phenol) [30,32,36]. Specifically, Rafael A. et al. reported that AgNPs can be obtained in the presence of functionalized host polymers (i.e., Novolak, poly (4-vinylphenol) (P4VP)). And this group reported that the easy migration of Ag^0 at above glass transition temperature (T_g) of the host polymer is important for the size and morphology control of the nanoparticles [36]. In other cases, there have been interesting reports of *in situ* synthesis of AgNPs in the photosensitive material systems (e.g., Diazonaphthoquinone (DNQ)-based photoresist/Ag composite, thiourea-stabilized Ag^+ complexes with bisphenol A diglycidyl ether (BADGE)) [11,15]. However, the DNQ-based material requires thermal baking at 190 °C, limiting their practical adaptation to soft polymer films, and the reduction of Ag^+ stabilized by thiourea requires special plasam equipment for Ag^+ reduction. Nonetheless, there is no doubt that such a direct patternable material system can be a simple and efficient approach to fabricating microelectrodes (sub-3 μm as line-width) *via* electroless plating methods. Hence, the lack of functional materials that enable *in situ* AgNPs formation at low temperatures and the straightforward fabrication of sub 3 μm metallic grids on soft polymer films still remains a challenge.

In the present study, it aims to solve the challenge through a

E-mail address: s21941@snu.ac.kr.

https://doi.org/10.1016/j.polymer.2020.123249
Received 15 September 2020; Received in revised form 8 November 2020; Accepted 18 November 2020
Available online 23 November 2020

bifunctional reactive building block whose enables versatile photosensitive resists and facilitates *in situ* synthesis of sub-20 nm AgNPs at low temperature. More specifically, the building block consists of two functional groups: one is *α,β*-unsaturated acryloyl group for photopolymerization under ultraviolet (UV) light and the other is a *para*-hydroxyl group protected by an acid labile group (Boc anhydride), which acts on Ag^+ reduction. Photosensitive resist not only enables *in situ* synthesis of AgNPs with great flexibility in choosing the process temperature, but also provides excellent process reliability during photolithographic patterning and electroless plating in strong alkaline solutions. Along with subsequent analysis, transparent conductive film with sub-3 μm metallic grids is demonstrated to explore direct patterning capabilities and adaptability to selective electroless plating.

2. Experimental

2.1. Materials

Hydroquinone (ReagentPlus®, 99%), di-*tert*-butyl decarbonate (Boc anhydride, ReagentPlus®, 99%), methacrylic anhydride (technical, ≥ 92%), zinc acetate dihydrate ($Zn(OAc)_2{\cdot}2H_2O$, ≥ 98%), silver nitrate ($AgNO_3$, ACS reagent, ≥ 99.0%), 1-hydroxycyclohexyl phenyl ketone (99%), (4-*tert*-butylphenyl)diphenylsulfonium triflate (99%), 4-(dimethylaminopyridine) (DMAP, ReagentPlus®, 99%), bisphenol A ethoxylated dimethacrylate (Mn ~ 1,700, contains 200 ppm monomethyl ether hydroquinone (MEHQ) as inhibitor), pentaerythritol tetraacrylate (contains 350 ppm MEHQ), tetrahydrofuran (anhydrous, for HPLC, ≥ 99.0%), propylene glycol monomethyl ether (PGME > 99.5%), formaldehyde (ACS reagent, 37 wt% in H_2O), sodium hydroxide solution (NaOH, 50 wt% in H_2O), ethyl acetate (anhydrous, 99.8%), *n*-hexane (anhydrous, 95%) were purchased from Sigma-Aldrich. Electroless copper plating solution (OPC-750 E'less M, ATS-Addcopper IW and ATS-Addcopper VR) was purchased from MK Chem & Tech (South Korea). PEN film (thickness: 125 μm) was received from Tekra, LLC. All chemicals are used as received.

2.2. Preparation of photosensitive solution

1.0 g of building block **3**, 1.0 g of 0.2 M $AgNO_3$ solution (PGME), 0.05 g of 1-hydroxycyclohexyl phenyl ketone (99%), and 0.015 g of (4-*tert*-butylphenyl)diphenylsulfonium triflate were dissolved in PGME and stored in the dark.

2.3. Preparation of photosensitive resist

First, a binder solution was prepared: 10.0 g of bisphenol A ethoxylate dimethacrylate, 2.5 g of pentaerythritol tetraacrylate, 2.5 g of building block **3**, 0.75 g of 1-hydroxycyclohexyl phenyl ketone (99%) (based on bisphenol A ethoxylate dimethacrylate), and 0.25 g of (4-*tert*-butylphenyl)diphenylsulfonium triflate (based on building block **3**) in PGME. Then, 15.0 g of 0.2 M $AgNO_3$ solution (PGME) was added to the as-prepared binder solution and stored in the dark.

2.4. Fabrication of copper patterns by electroless plating

As-prepared photosensitive resist was spun-cast on a cleaned PEN film (thickness: 125 μm) at a rate of 2000 rpm for 10 s to yield 5 μm thick resist film. After pre-baking at 60 °C for 30 s, the resist film was exposed to *i*-line (Suss Microtec MJB4 Precision Mask Aligner, ~92 mJ/cm^2) under a photomask and rinsed with PGME to remove non-crosslinked resist. The resist was further performed post-exposure baking at 120 °C for 10 min (note that the exposed area becomes light yellowish due to created AgNPs). Then, the substrate was immersed into an electroless copper plating solution with air agitation as a rate of 2.5 *l*/min (note that operating temperature was set to 47 °C with adjusted pH 11.5–12). After 10 min, the substrate was rinsed with water to remove residual reducing agents and dried at vacuum oven (80 °C) prior to further characterization.

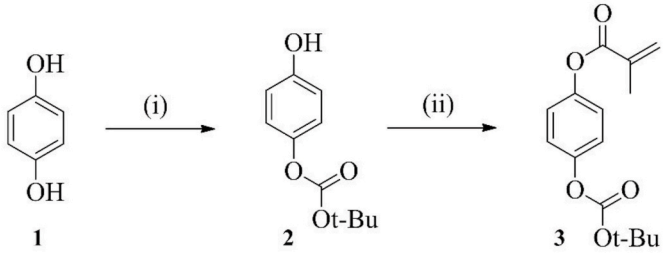

Scheme 1. Synthesis of building block **3**. (i) 1.05 equvi Boc anhydride, 40 mol % Zn $(OAc)_2$ dihydrate, anhydrous tetrahydrofuran (THF), 70 °C, 12 h, (ii) 1.1 equvi methacrylic anhydride, 20 mol % 4-(Dimethylaminopyridine) (DMAP), anhydrous THF, 70 °C, 6 h.

2.5. Characterization

Absorption and optical transmittance were measured with Shimadzu UV-1800. Measurement of sheet resistance was performed by 4 point probe (M4P_302_System, MS TECH). FT-IR was performed on a PerkinElmer. Film thickness was measured by DektakXT (BRUKER). Karl Suss MJB3 UV400 mask aligner was used for micro-patterning. NMR spectroscopy was performed at 700 MHz (Bruker, Model: AVANCEIII 700). SEM and EDS measurements were performed by JSM-7600F (JEOL, accelerating voltage 0.1–30 kV). AFM measurement was performed by NanoWizard Ultra Speed (JPK Instruments). XRD measurement was performed by D8 ADVANCE (Bruker). TEM measurement was performed by JEM-3010 (JEOL, accelerating voltage 100–300 kV).

3. Results and discussion

The bifunctional building block **3** was derived from poly (4-vinylphenol) that enables sub-10 nm AgNPs and improves adhesion to copper metals [43–45]. Successful synthesis is depicted in Scheme 1. Hydroquinone **1** (90.82 mmol) as a starting material, Boc anhydride (95.34 mmol) and $Zn(OAc)_2$ dihydrate (36.33 mmol) as a catalyst were dissolved in anhydrous tetrahydrofuran (THF) at once. After reaction (12 h at 70 °C), white solid **2** (83% yield) was given by recrystallization with ethyl acetate/hexane (1:10, v/v%). The obtained intermediate **2** was further reacted with methacrylic anhydride (82.92 mmol) to give the *α,β*-unsaturated acryloyl group represented by **3** (light yellowish liquid, 98% yield). Note that no difficulties were explored during the entire synthesis, and proton nuclear magnetic resonance (^1H NMR) spectroscopy is shown in Fig. S1.

Fig. 1a represents a newly designed one-pot multi-reactions enabling *in situ* synthesis of AgNPs. Step 1 (one-pot photoreactions) involves the photopolymerization of building block **3** and the release of triflate acid from the photoacid generator (referred to as PAG), and subsequent thermal baking (step 2) involves cleavage of Boc groups, Ag^+ reduction and nucleation. In particular, the free hydroxyl groups after deprotection act on Ag^+ reduction, and subsequent nucleation can be facilitated through easy migration of Ag^0 in the rubbery state of polymer during thermal baking [36]. For proof of concept, photosensitive solution (see Experimental Section) was prepared by dissolving **3** in propylene glycol monomethyl ether (PGME) along with $AgNO_3$, photoinitiator (PI) **5** and PAG **6**. Note that the dissolved $AgNO_3$ can presumably coordinate with hydroxyl group oxygen or carbonyl group oxygen to form Ag^+ complexes (see Fig. 1a) [35]. Each step was monitored by Fourier Transform Infrared (FT-IR) spectroscopy to confirm polymerization **6** of each building block by radicals and then to find the time-dependent Boc cleavage at 120 °C. The FT-IR spectra (see Fig. 1b) shows a set of new peaks at 1757 cm^{-1} and 1736 cm^{-1}, corresponding to the two ester groups of **3**. The two vague broad bands ranging from

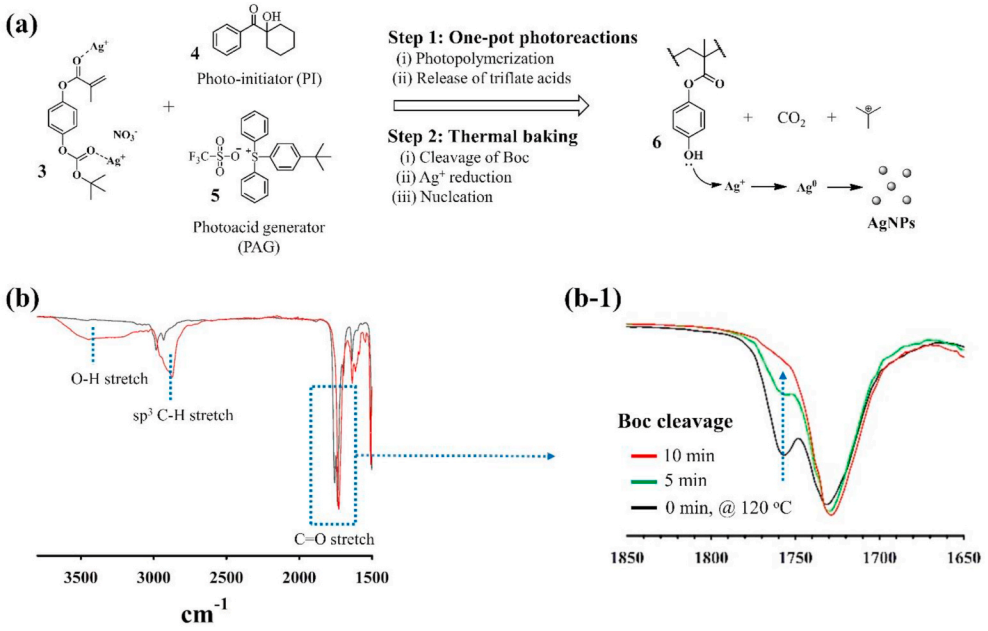

Fig. 1. (a) Designed reaction steps for *in situ* synthesis of AgNPs with **3**, (b) FT-IR spectroscopy: before and after Boc cleavage, [Note that the photosensitive solution was cured under UV light (365 nm, 92 mJ/cm^2) after spin-casting on a glass, then thermally baked at 120 °C for 10 min], polymerized building blocks (black) and 10 min thermal baking at 120 °C (red), (b-1) FT-IR spectroscopy: progress of Boc cleavage over baking time at 120 °C. (For interpretation of the references to colour in this figure legend, the reader is referred to the Web version of this article.)

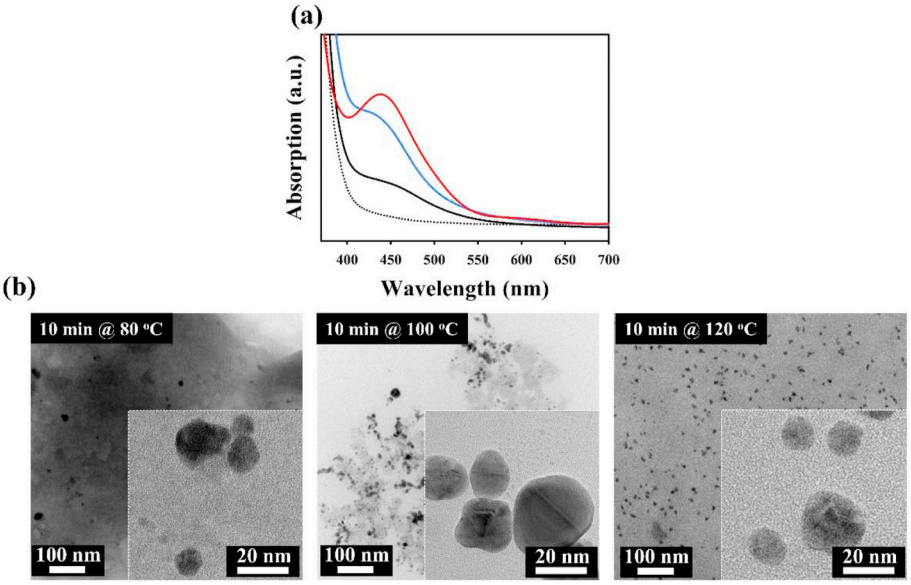

Fig. 2. (a) Characterization of surface plasmon absorption of *in situ* synthesized AgNPs in cured building block matrices, [note that curing was performed by UV light (365 nm, 92 mJ/cm^2)], control (black dotted line) versus experimental matrices containing $AgNO_3$, solid black line: baked at 80 °C, solid blue line: baked 100 °C, solid red line: baked at 120 °C, and (b) corresponding transmission electron microscopy (TEM) showing the morphology and distribution of AgNPs in the matrices. (For interpretation of the references to colour in this figure legend, the reader is referred to the Web version of this article.)

2700 cm^{-1} to 3700 cm^{-1} represent the sp^3 C–H stretch and the aromatic O–H stretch, respectively. Thus, the obtained data supports the complete polymerization and successful cleavage of Boc group. More specifically, the progress of Boc cleavage was monitored and shown in Fig. 1b–. In addition, differential scanning calorimetry (DTA) analysis shows that the polymerized building block is completely melted at 171 °C (see Fig. S4).

Successful *in situ* synthesis of AgNPs can be confirmed by localized surface plasmon resonances (LSPRs). In principle, LSPRs of AgNPs exhibit strong and broad optical absorption bands depending on size, morphology and many reasons [1–3]. Specially, the surface plasmonic absorption bands of AgNPs (sub-40 nm) embedded in the matrix appear at around 410 nm and 430 nm depending on the baking temperature and the T_g of the matrix [36]. In Fig. 2a, the λ_{max} of LSPR appears at around 430–440 nm when the cured building block matrices are baked at 80 °C, 100 °C and 120 °C, respectively. Considering the small variation in film thickness (500 ± 3 nm), the changes in intensity of plasmon absorption could be due to the distribution and concentration of AgNPs in the matrix. As shown in Fig. 2b, it appears to be supported by transmission electron microscopy (TEM) representing the distribution of AgNPs with the applied baking temperatures. Regarding the nanoparticle size, it is widely accepted that the nucleation and growth of small nanoparticles (i.e., sub 20 nm) are kinetically favored at low temperatures. In this study, AgNPs smaller than 20 nm are observed in all experimental conditions, but particulary the matrix baked at 120 °C shows much uniform distributions of sub-20 nm AgNPs. Thus, the building block appears to promote kinetically favored nucleation and growth, as well as helping AgNPs remain isolated [30,32,36].

It is well known that AgNPs are involved in a variety of chemical oxidation and reduction [8,9], and other studies have demonstrated that the AgNPs as a palladium (Pd) substitution show high potential for highly efficient, low-cost electroless metal plating [11,15,25–29,39]. In the present work, a photosensitive solution for *in situ* synthesis of AgNPs was applied to electroless copper plating. First, the photosensitive

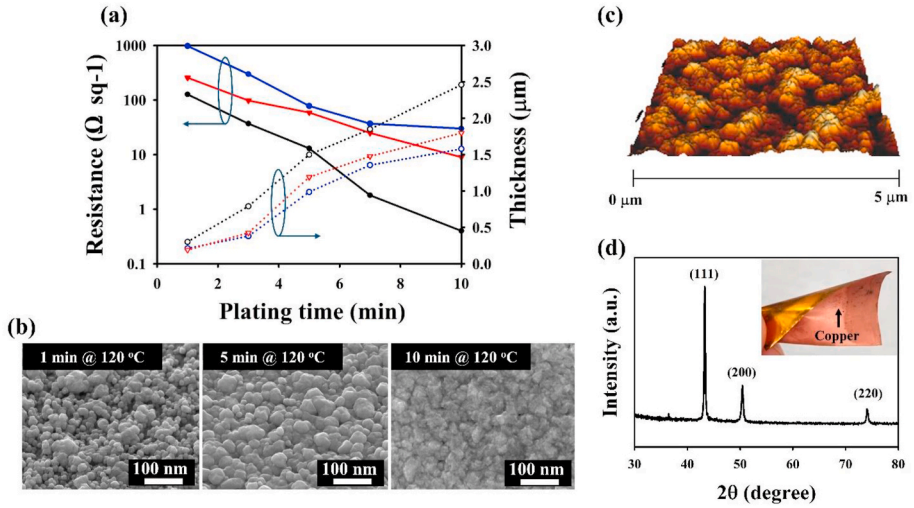

Fig. 3. (a) The cross-sectional characterization of electrical resistance (Ω/sq), thickness and plating time: solid black and dotted lines (baked at 120 °C), solid red and dotted lines (baked at 100 °C), solid blue and dotted lines (baked at 80 °C), respectively, (b) SEM of the copper surface over time at 120 °C and (c) corresponding AFM after 10 min deposition (R_t (peak-to-valley): around 60 nm), (d) XRD spectra of copper grain after 10 min deposition (the inset: copper-deposited PEN film). (For interpretation of the references to colour in this figure legend, the reader is referred to the Web version of this article.)

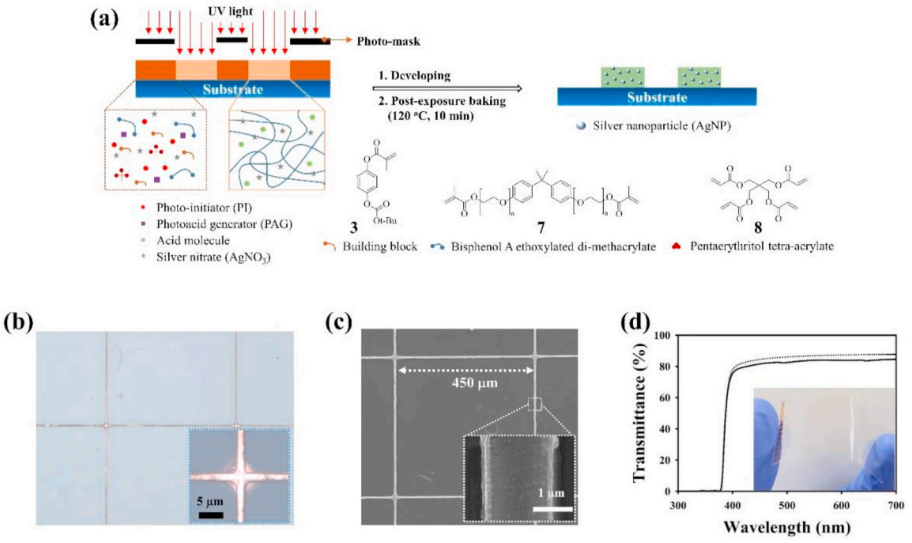

Fig. 4. (a) Diagram of selective electroless copper plating through direct patternable photosensitive resist, (b) optical microscopy of sub-3 μm copper grids on PEN film and (c) corresponding SEM, (d) optical transmittance at 550 nm (the inset: PEN film with sub-3 μm copper grids), black dotted line: bare PEN film, black solid line: PEN film with sub-3 μm copper grids.

solution was spun-casted onto a PEN substrate, followed UV exposure (365 nm, 92 mJ/cm^2) and thermal baking at 80 °C, 100 °C and 120 °C, repectively. As mentioned, since the size and concentration of AgNPs depend on the applied baking temperatures, the changes in electrical resistance (Ω/sq) of each substrate was monitored over time. As shown in Fig. 3a, the electrical resistance of the substrate baked at 120 °C decreases almost exponentially, reaching its lowest value (0.6 Ω/sq) within 10 min of plating time. Others, on the other hand, exhibit rather high values (8.6 Ω/sq and 56.3 Ω/sq, respectively). The thickness of corresponding substrates increases almost linearly, reaching 1.5–2.5 μm over time. As a result, cross-sectional analysis indicates that copper deposition is dependent on the size and concentration of AgNPs. In addition, the corresponding scanning electron microscope (SEM) confirms that the deposited Cu grains become steadily dense over the plating time (see Fig. 3b), so that dense contact between adjacent grains reduces the electrical resistance. And the characterized surface images (*via* atomic force microscopy (AFM)) also confirms that the Cu-deposited surface has a high roughness (R_t (peak-to-valley: 60 nm). In addition to the XRD pattern having nearly identical results (mainly three Bragg diffraction peaks corresponding to (111), (200) and (220) crystal planes of Cu, respectively [15,44], the EDS analysis (see Fig. S2) shows that the deposited area is mainly Cu atoms (calculated as > 90 wt%) with trace amounts of Ag atoms (calculated as < 2 wt%).

As a potential application, the present work was applied to transparent conducting films consisting of metal grids [37–42,52–56]. One of the key indicators of the metal grid-based conductive film is the invisibility of the metal grid, so it is important to achieve sub-3 μm metal grids. Therefore, photosensitive resists should ensure sub-2 μm (as line-width) resist patterns, as well as high chemical resistance to strong alkaline solutions (pH 10–12 for common electroless plating). Thus, photosensitive solution was further formulated with commercially available curable monomers (**7** and **8**) (see Experimental Section). Note that PGME is a good solvent effectively dissolving all components without sediment. Besides, curable monomers improve the mechanical stability and chemical resistance of the resist pattern, consequently preventing pattern collapse and peeling. Fig. 4a is a diagram of the direct pattering procedure and selective *in situ* synthesis of AgNPs. After spin-casting the photosensitive resist on PEN substrate, the resist was exposed to UV light (365 nm, 92 mJ/cm^2) under a photomask. After developing by PGME for 30 s, fine resist patterns were successfully

formed on PEN substrate. As shown in Fig. S3, the attained 2 μm resist pattern confirms no pattern collapse and peeling during the photolithography process. Subsequently, as-prepared resist pattern was thermally baked at 120 °C for 10 min, then immersed in a container filled with a commercial Cu plating solution to perform electroless plating (see Experimental Section). As shown in Fig. 4b and corresponding SEM (Fig. 4c), the resulting sub-3 μm metal grids indicate that the photosensitive resist ensures excellent process reliability in strong alkaline solution. The optical transmittance is also another key indicator, therefore it was confirmed by UV–vis spectroscopy. As seen in Fig. 4d and the inset, optical transmittance (T_{500}) was well preserved despite the small decrease (83% at 550 nm, (decreased by 2%)).

4. Conclusions

In summary, this work presents a bifunctional building block and photosensitive resist that enables *in situ* synthesis of sub-20 nm AgNPs. More specifically, the bifunctional building block, which acts on both photopolymerization and Ag^+ reduction, can be prepared by simple organic synthesis skills. The plasmonic absorption after baking at 80–120 °C proves successful synthesis of AgNPs embedded in the matrix. The *in situ* synthesized AgNPs enabled Pd-free electroless Cu plating, and the electrical resistance decreases almost exponentially, reaching its lowest value (0.6 Ω/sq) within 10 min of plating time. In addition, the attained 2 μm resist pattern promised excellent process reliability by preventing pattern collapse and peeling during photolithographic patterning process and plating in strong alkaline solutions (pH 10–12). A result, the approach and results of this study not only provide a simple and effective chemical means of structuring sub-3 μm metal grids *via* Pd-free electroless plating methods on a soft substrate, but also a great opportunity for process temperature selection. As the following studies, high-performance of sub 3 μm electrodes and applications to flexible optoelectronics and stretchable devices are still ongoing.

Declaration of competing interest

The authors declare that they have no known competing financial interests or personal relationships that could have appeared to influence the work reported in this paper.

Appendix A. Supplementary data

Supplementary data to this article can be found online at https://doi.org/10.1016/j.polymer.2020.123249.

References

[1] A. Campos, N. Troc, E. Cottancin, M. Pellarin, H.C. Weissker, J. Lerme, M. Kociak, M. Hillenkamp, Plasmonic quantum size effects in silver nanoparticles are dominated by interfaces and local environments, Nat. Phys. 15 (2019) 275.

[2] S. Peng, J.M. McMahon, G.C. Schatz, S.K. Gray, Y. Sun, Reversing the size-dependence of surface plasmon resonances, Proc. Natl. Acad. Sci. U.S.A. 107 (2010) 14530.

[3] N. Fang, H. Lee, C. Sun, X. Zhang, Sub-diffraction-limited optical imaging with a silver superlens, Science 308 (2005) 534.

[4] E. Ozbay, Plasmonics: merging photonics and electronics at nanoscale dimensions, Science 311 (2006) 189.

[5] S. Agnihotri, S. Mukherji, S. Mukherji, Size-controlled silver nanoparticles synthesized over the range 5-100 nm using the same protocol and their antibacterial efficacy, RSC Adv. 4 (2014) 3974.

[6] A. Loiseau, V. Asila, G. Boitel-Aullen, M. Lam, M. Salmain, S. Boujday, Silver-based plasmonic nanoparticles for and their use in biosensing, Biosensors 9 (2019) 78.

[7] H. Haidari, N. Goswami, R. Bright, Z. Kopecki, A.J. Cowin, S. Grag, K. Vasilev, The interplay between size and valence state on the antibacterial activity of sub-10 nm silver nanoparticles, Nanoscale Adv. 1 (2019) 2365.

[8] S. Cao, F. Tao, Y. Tang, Y. Li, J. Yu, Size-and shape-dependent catalytic performances of oxidation and reduction reaction on nanocatalysts, Chem. Soc. Rev. 45 (2016) 4747.

[9] Y. Zhou, C. Jin, Y. Li, W. Shen, Dynamic behavior of metal nanoparticles for catalysis, Nano Today 20 (2018) 101.

[10] S. Ghosh, Electroless copper deposition: a critical review, Thin Solid Films 669 (2019) 641.

[11] A. Ryspayeva, T.D.A. Jones, M.N. Esfahani, M.P. Shuttleworth, R.A. Harris, R. W. Kay, M.P.Y. Desmulliez, J. Marques-Hueso, Selective electroless copper deposition by using photolithographic polymer/Ag nanocomposite, IEEE Trans. Electron. Dev. 66 (2019) 1843.

[12] Q. Si Shao, R.C. Bai, Z.Y. Tang, Y.F. Gao, J.L. Sun, M.S. Ren, Durable electroless Ni and Ni-P-B plating on aromatic polysulfonamide (PSA) fibers with different performances via chlorine-aided silver activation strategy, Surf. Coating. Technol. 302 (2016) 185.

[13] Y. Shacham-Diamand, T. Osaka, Y. Okinaka, A. Sugiyama, V. Dubin, 30 years of electroless plating for semiconductor and polymer micro-systems, Microelectron. Eng. 132 (2015) 35.

[14] J. Cai, M. Zhang, Z. Sun, C. Zhang, C. Liang, A. Khan, X. Ning, H. Ge, S.P. Feng, W. D. Li, Highly-facile template-based selective electroless metallization of micro- and nanopatterns for plastic electronics and plasmonics, J. Mater. Chem. C 7 (2019) 4363.

[15] Y. Wang, Y. Hong, G. Zhou, W. He, Z. Gao, S. Wang, C. Wang, Y. Chen, Z. Weng, Y. Wang, Compatile Ag^+ complex-assisted ultrafine copper pattern deposition on poly(ethylene terephthalate) film with micro inkjet printing, ACS Appl. Mater. Interfaces 11 (2019) 44811.

[16] F.T. Zhang, L. Xu, J.H. Chen, B. Zhao, X.Z. Fu, R. Sun, Q. Chen, C.P. Wong, Electroless deposition metals on poly(dimethylsiloxane) with strong adhesion as flexible and stretchable conductive materials, ACS Appl. Mater. Interfaces 10 (2018) 2075.

[17] Y.C. Liao, Z.K. Kao, Direct writing patterns for electroless plated copper thin film on plastic substrates, ACS Appl. Mater. Interfaces 4 (2012) 5109.

[18] S.J. Park, T.J. Ko, J. Yoon, M.W. Moon, K.H. Oh, J.H. Han, Copper circuit patterning on polymer using selective surface modification and electroless plating, Appl. Surf. Sci. 396 (2017) 1678.

[19] A. Sahasrabudhe, H. Dixit, R. Majee, S. Bhattacharyya, Value added transformation of ubiquitous substrates into highly efficient and flexible electrodes for water splitting, Nat. Commun. 9 (2018) 2014.

[20] X. Lin, M. Wu, L. Zhang, D. Wang, Superior stretchable conductors by electroless plating of copper on knitted fabrics, ACS Appl. Electron. Mater. 1 (2019) 397.

[21] C. Wu, X. Tang, L. Gan, W. Li, J. Zhang, H. Wang, Z. Qin, T. Zhang, T. Zhou, J. Huang, C. Xie, D. Zeng, High-adhesion stretchable electrode via cross-linked intensified electroless deposition on a biomimetic elastomeric micropore film, ACS Appl. Mater. Interfaces 11 (2019) 20535.

[22] M. Hu, Q. Guo, T. Zhang, S. Zhou, J. Yang, SU-8-induced strong bonding of polymer ligands to flexible substrates via in situ cross-linked reaction for improved surface metallization and fast fabrication of high-quality flexible circuits, ACS Appl. Mater. Interfaces 8 (2016) 4280.

[23] Y. Zhang, S.W. Ng, X. Lu, Z. Zheng, Solution-processed transparent electrodes for emerging thin-film solar cells, Chem. Rev. 120 (2020) 2049.

[24] Y. Yang, W. Liu, Q. Huang, X. Li, H. Ling, J. Ren, R. Sun, J. Zou, X. Wang, Full solution-processed fabrication of conductive hybrid paper electrodes for organic electronics, ACS Sustain. Chem. Eng. 8 (2020) 3392.

[25] P. Li, Y. Zhang, Z. Zheng, Polymer-assisted metal deposition (PAMD) for flexible and wearable electronics: principle, materials, printing, and devices, Adv. Mater. 31 (2019), 1902987.

[26] L. Shen, Y. Zhang, W. Yu, R. Li, M. Wang, Q. Gao, J. Li, H. Lin, Fabrication of hydrophilic and antibacterial poly(vinylidene fluoride) based separation membranes by a novel strategy combining radiation grafting of poly(acrylic acid) (PAA) and electroless nickel plating, J. Colloid Interface Sci. 543 (2019) 64.

[27] B. Vasconcelos, K. Vediappan, J.C. Oliveira, C. Fonseca, Mechanically robust silver coatings prepared by electroless plating on thermoplastic polyurethane, Appl. Surf. Sci. 443 (2018) 39.

[28] F.M. Wisser, B. Schumm, G. Mondin, J. Grothe, S. Kaskel, Precursor strategies for metallic nano- and micropatterns using soft lithography, J. Mater. Chem. C 3 (2015) 2717.

[29] X. Sun, L. Zhang, S. Tao, Y. Yu, S. Li, H. Wang, J. Qiu, A general surface swelling-induced electroless deposition strategy for fast fabrication of copper circuits on various polymer substrates, Adv. Mater. Intefaces 4 (2017) 1700052.

[30] J.L. Hernandez-Pinero, M. Terron-Rebolledo, R. Foroughbakhch, S. Moreno-Limon, M.F. Melendrez, F.S. Pomar, E. Perez-Tijerina, Effect of heating rate and plant species on the size and uniformity of silver nanoparticles synthesized using aromatic plant extracts, Appl. Nanosci. 6 (2016) 1183.

[31] G.V. Ramesh, S. Porel, T.P. Radhakrishnan, Polymer thin films embedded with in situ grown metal nanoparticles, Chem. Soc. Rev. 38 (2009) 2646.

[32] Q. Liu, N. Chen, S. Bai, W. Li, Effect of silver nitrate on the thermal processability of poly(vinyl alcohol) modified by water, RSC Adv. 8 (2018) 2804.

[33] K. Kashihara, Y. Uto, T. Nakajima, Rapid *in situ* synthesis of polymer-metal nanocomposite films in several seconds using a CO_2 laser, Sci. Rep. 8 (2018) 14719.

[34] S. Rifai, C.A. Breen, D.J. Solis, T.M. Swager, Facile *in situ* silver nanoparticle formation in insulating porous polymer matrices, Chem. Mater. 18 (2006) 21.

[35] Y. Gan, S. Bai, S. Hu, X. Zhao, Y. Li, Reaction mechanism of thermally-induced electric conduction of poly(vinyl alcohol)-silver nitrate hybrid films, RSC Adv. 6 (2016) 56728.

[36] R. Abargues, K. Abderrafi, E. Pedrueza, R. Gradess, J. Marques-Hueso, J.L. Valdes, J. Martinez-Pastor, Optical properties of different polymer thin films containing *in situ* synthesized Ag and Au nanoparticles, New J. Chem. 33 (2009) 1720.

[37] H.B. Lee, W.Y. Jin, M.M. Ovhal, N. Kumar, J.W. Kang, Flexible transparent conducting electrodes based on metal meshes for organic optoelectronic device applications: a review, J. Mater. Chem. 7 (2019) 1087.

[38] S. Varagnolo, J. Lee, H. Amari, R.A. Hatton, Selective deposition of silver and copper films by condensation coefficient modulation, Mater. Horiz. 7 (2020) 143.

[39] Y.S. Oh, D.Y. Choi, H.J. Sung, Direct imprinting of thermally reduced silver nanoparticles via deformation-dirven ink injection for high-performance, flexible metal grid embedded transparent conductors, RSC Adv. 5 (2015) 64661.
[40] K. Zilberberg, T. Riedl, Metal-nanostructures - a modern and powerful platform to create transparent electrodes for thin-film photovoltaics, J. Mater. Chem. A. 4 (2016) 14481.
[41] S. Han, Y. Chae, J.Y. Kim, Y. Jo, S.S. Lee, S.H. Kim, K. Woo, S. Jeong, Y. Chol, S. Y. Lee, High-performance solution-processable flexible and transparent conducting electrodes with embedded Cu mesh, J. Mater. Chem. C. 6 (2018) 4389.
[42] L. Li, B. Zhang, B. Zou, R. Xie, T. Zhang, S. Li, B. Zheng, J. Wu, J. Weng, W. Zhang, W. Huang, F. Huo, Fabrication of flexible transparent electrode with enhanced conductivity from hierarchical metal grids, ACS Appl. Mater. Interfaces 9 (2017) 39110.
[43] Z. Wang, H.C. Yang, F. He, S. Peng, Y. Li, L. Shao, S.B. Darling, Mussel-inspired surface engineering for water-remediation materials, Matter 1 (2019) 115.
[44] P.K. Forooshani, B.P. Lee, Recent approaches in designing bioadhesive materials inspired by mussel adhesive protein, J. Polym. Sci. Polym. Chem. 55 (2017) 9.
[45] L. Zhao, D. Chen, W. Hu, Patterning of metal films on arbitrary substrates by using polydopamine as a UV-sensitive catalytic layer for electroless deposition, Langmuir 32 (2016) 5285.
[46] G.V. Ramesh, S. Porel, T.P. Radhakrishnan, Polymer thin films embedded with in situ grown metal nanoparticles, Chem. Soc. Rev. 38 (2009) 2646.
[47] Ch Venkata Reddy, I. Neelakanta Reddy, K. Ravindranadh, Kakarla Raghava Reddy, Nagaraj P. Shetti, D. Kim, J. Shim, Tejraj M. Aminabhavi, Copper-doped ZrO_2 nanoparticles as high-performance catalysts for efficient removal of toxic organic pollutants and stable solar water oxidation, J. Environ. Manag. 260 (2020) 110088.
[48] M. Srinivas, Ch Venkata Reddy, Raghava Reddy Kakarla, Nagaraj P. Shetti, M. S. Reddy, V Raghu Anjanapura, Novel Co and Ni metal nanostructures as efficient photocatalysts for photodegradation of organic dyes, Mater. Res. Express 6 (2019), 125502.
[49] Nagaraj P. Shetti, Deepti S. Nayak, Shweta J. Malode, Kakarla Raghava Reddy, Shyam S. Shukla, Tejraj M. Aminabhavi, Electrochemical behavior of flufenamic acid at amberlite XAD-4 resin and silver-doped titanium dioxide/amberlite XAD-4 resin modified carbon electrodes, Colloids Surf., B 177 (2019) 407.
[50] Ch Venkata Reddy, I. Neelakanta Reddy, V.V.N. Harish, Kakarla Raghava Reddy, Nagaraj P. Shetti, Jaesool Shim, Tejraj M. Aminabhavi, Efficient removal of toxic organic dyes and photoelectrochemical properties of iron-doped zirconia nanoparticles, Chemosphere 239 (2020) 124766.
[51] Ch Venkata Reddy, I. Neelakanta Reddy, Bhargav Akkinepally, Kakarla Raghava Reddy, Jaesool Shim, Synthesis and photoelectrochemical water oxidation of (Y, Cu) codoped α-Fe_2O_3 nanostructure photoanode, J. Alloys Compd. 814 (2020), 152349.
[52] Kakarla Raghava Reddy, Kwang-Pill Lee, Anantha Iyenger Gopalan, Self-assembly directed synthesis of poly (ortho-toluidine)-metal (gold and palladium) composite nanospheres, J. Nanosci. Nanotechnol. 7 (2007) 3117.
[53] Kakarla Raghava Reddy, Byung Cheol Sin, Chi Ho Yoo, Daewon Sohn, Youngil Lee, Coating of multiwalled carbon nanotubes with polymer nanospheres through microemulsion polymerization, J. Colloid Interface Sci. 340 (2009) 160.
[54] Kakarla Raghava Reddy, Kwang-Pill Lee, Youngil Lee, Anantha Iyengar Gopalan, Facile synthesis of conducting polymer–metal hybrid nanocomposite by in situ chemical oxidative polymerization with negatively charged metal nanoparticles, Mater. Lett. 62 (2008) 1815.
[55] Kakarla Raghava Reddy, Byung Cheol Sin, Kwang Sun Ryu, Jin-Chun Kim, Hoeil Chung, Youngil Lee, Conducting polymer functionalized multi-walled carbon nanotubes with noble metal nanoparticles: synthesis, morphological characteristics and electrical properties, Synth. Met. 159 (2009) 595.
[56] B.S. Dakshayini, Kakarla Raghava Reddy, Amit Mishra, Nagaraj P. Shetti, Shweta J. Malode, Soumen Basu, S. Naveen, Anjanapura V. Raghu, Role of conducting polymer and metal oxide-based hybrids for applications in amperometric sensors and biosensors, Microchem. J. 147 (2019) 7.